J. Radiat. Res., 48: Suppl., A61-A74 (2007)

Integration of Enhanced Optical Tracking Techniques and Imaging in IGRT

Guido BARONI[1]*, Marco RIBOLDI[1], Maria Francesca SPADEA[1], Barbara TAGASTE[2], Cristina GARIBALDI[2], Roberto ORECCHIA[3,4] and Antonio PEDOTTI[1]

Patient setup/Optical tracking/IGRT/Treatment surveillance.

In external beam radiotherapy, modern technologies for dynamic dose delivery and beam conformation provide high selectivity in radiation dose administration to the pathological volume. A comparable accuracy level is needed in the 3-D localization of tumor and organs at risk (OARs), in order to accomplish the planned dose distribution in the reality of each irradiation session.

In-room imaging techniques for patient setup verification and tumor targeting may benefit of the combined daily use of optical tracking technologies, supported by techniques for the detection and compensation of organ motion events. Multiple solutions to enhance the use of optical tracking for the on-line correction of target localization uncertainties are described, with specific emphasis on the compensation of setup errors, breathing movements and non-rigid deformations. The final goal is the implementation of customized protocols where appropriate external landmarks, to be tracked in real-time by means of non-invasive optical devices, are selected as a function of inner target localization.

The presented methodology features high accuracy in patient setup optimization, also providing a valuable tool for on-line patient surveillance, taking into account both breathing and deformation effects. The methodic application of optical tracking is put forward to represent a reliable and low cost procedure for the reduction of safety margins, once the patient-specific correlation between external landmarks and inner structures has been established. Therefore, the integration of optical tracking with in-room imaging devices is proposed as a way to gain higher confidence in the framework of Image Guided Radiation Therapy (IGRT) treatments.

INTRODUCTION

High accuracy in the 3-D localization of target volume and organs at risk (OARs) in external radiotherapy is a crucial issue, particularly when hypo-fractionated treatments and dose escalation techniques are used aiming at improving tumor local control.[1)] High-precision radiation treatment plans are based on the recent development of technologies for dynamic dose delivery and beam conformation, which provide the highest geometric selectivity in radiation dose administration to the pathological volume, with the contemporary maximal sparing of the surrounding healthy structures. In these cases, treatment plan optimization relies on high-resolution 3-D imaging modalities for the design of highly conformal dose distributions, with millimeter-scale tolerances around the target.[2)]

A comparable accuracy level is needed in the 3-D localization of tumor and OARs at each irradiation session, in order to accomplish the planned dose distribution. High accuracy in tumor localization is the necessary prerequisite to ensure the effective repeatability in the irradiation setup at each fraction, in terms of the relative position of tumor and OARs with respect to the radiation beam. Daily variability in the 3-D position of relevant internal structures is due to several reasons:

- uncertainties in patient positioning (setup errors)
- morphologic changes of the irradiated district
- physiologic (breathing) and/or random patient movements
- organ motion effects.

In current clinical practice, geometrical uncertainties are faced by adding safety margins of surrounding healthy tissue to the clinical target volume (CTV): the resulting enlarged

*Corresponding author: Phone: +39-02-2399-3349,
Fax: +39-02-2399-3360,
E-mail: guido.baroni@polimi.it

[1]TBMLab-Department of Bioengineering, Politecnico di Milano University, Piazza Leonardo da Vinci 32, I-20133 Milano, Italy; [2]Medical Physics, European Institute of Oncology, Via Ripamonti 435, 20141 Milano, Italy; [3]Radiotherapy Division, European Institute of Oncology, Via Ripamonti 435, 20141Milano, Italy; [4]Istituto di Scienze Radiologiche, Polo Universitario H S. Paolo,Via Rudini 8, I-20142 Milano, Italy.

volume is commonly referred to as planned target volume (PTV). Additional margins of healthy tissue encompass both the uncertainties due to patient setup (setup margin, SM) and the ones related to inner movements of the irradiation target (internal margin, IM).[3] This conservative approach is imposed by the lack of a systematic quantitative verification of the irradiation setup, and reduces the therapeutic potentialities of complex irradiation techniques.[4]

Conventional procedures for patient setup in radiotherapy are based on the manual alignment of skin landmarks (tattoos) by means of laser-projected reference laser lines, under a core rigid-body assumption.[5,6] Manual alignment techniques do not provide any quantitative measure and/or technical documentation of setup accuracy, which is highly dependent on the operator's skill. In-room imaging techniques (orthogonal X-rays, cone beam CT, ultrasound) can be exploited to verify the absolute localization of tumor and OARs before the irradiation in an image-guided approach (Image Guided Radiation Therapy, IGRT).[7] Nevertheless, the application of image guidance in clinical practice is limited by the high costs and by the related increase in total treatment time. As a matter of fact, systematic image-guided patient positioning is hardly applicable in the reality of a modern radiotherapy division where hundreds of patients are treated daily. Furthermore, image guidance usually yields the verification of tumor localization before the irradiation, lacking of real-time monitoring during treatment. The manual patient setup can be defined basically an *outside-in* methodology, meaning that no site and patient-specific design criteria, based on treatment planning data, are applied to the selection of external features for patient positioning. Patient setup is performed on the basis of external landmarks in a standardized manner, and in-room imaging techniques, when available, represent the only methodological basis of setup accuracy check.

In recent years, optical tracking systems have been proposed in radiotherapy for the implementation of computer-aided patient positioning procedures.[8] Opto-electronic systems based on infrared detection are commonly used for the stereo-photogrammetric reconstruction of a set of physical control points located on patient's skin (skin markers). The real-time comparison between control points position with a corresponding reference configuration, defined at treatment simulation, provides the quantitative evaluation of patient localization errors. Moreover, data analysis procedures can be applied to highlight the different factors affecting the accuracy of the irradiation setup, such as operator-dependant positioning errors, patient breathing and random movements.[5,6] Infrared technologies combine sub-millimeter localization accuracy, minimal invasiveness and inertia towards ionizing radiations, thus emerging as the benchmark solution for skin marker tracking in radiotherapy.[9] Alternatively, 3-D video systems based on speckle projection allow to capture the full 3-D surface information in a single snapshot (10 *ms*), though stereo-photogrammetric reconstruction time bounds the frame-rate capture to few (5–7) *Hz*.[10,11] These systems output 3-D geometrical representations of patient surface that are essentially composed of triangular tiles; surface representations acquired at each treatment fraction are compared to a preset reference model within a user defined region of interest (ROI).[10] Rigid registration is used to evaluate the correction transformation maximizing surface fitting: the couch movements to be performed for correcting patient positioning can be calculated in few seconds. These 3-D camera systems can easily detect shape changes and/or monitor the whole surface motion due to respiration, though they are not suitable for real-time applications.

In this work, we review an *inside-out* paradigm for patient setup, by reviewing methodological and clinical developments aiming at optimizing the modalities under which the treatment is planned and realized. This approach consists of exploiting treatment planning data as a way to customize the selection of the external features to be used for in-room patient setup definition and verification. Specific attention is given to the application of the *inside-out* paradigm in the framework of computer aided patient setup procedures, guided by modern technologies for optical tracking. The applicability of point-based and surface-based patient localization techniques is described, with particular emphasis on enhancing the flow of positioning data information for patient setup procedures that purposely take into account respiration and surface deformation. Furthermore, the use of external landmarks for the estimate of the internal target position is discussed, aiming at the optimal placement of surface markers on one hand, and at the application of robust stereotactic localization procedures on the other. Finally, the correlation of external markers position and internal target localization is investigated, with reference to potential integration with imaging techniques and clinical protocols for the compensation of breathing movements.

METHODS AND MATERIALS

In this section, methodologies and protocols applied for patient position optical tracking will be presented. Clinical studies were performed in cooperation with the Radiotherapy Division of the European Institute of Oncology (Milan, Italy), where two localization systems (ELITE, BTS, S.p.a. Milan, Italy), in a two TV-cameras (TVC) configuration, were installed at the CT and therapy unit, respectively. Algorithm implementation and testing were carried out at the TBMLab (Laboratory of Biomedical Technologies), Department of Bioengineering, Politecnico di Milano University (Milano, Italy).

Optical point-based techniques for patient position monitoring

The infrared optical 3D tracking of surface markers was

applied to quantify inter-fractional setup variability on 51 patients treated in prone or supine position. High-precision radiotherapy (extra-cranial stereotactic radiotherapy) was selected as the reference clinical protocol.[12] The configuration of external control points (ranging in number from 5 to 8) was defined at the CT unit for each patient. Markers were placed on the patient before the acquisition of the CT slices and their reference coordinates were used for stereotactic treatment planning. The optical system installed in the simulation room was used to record marker reference positions, which were averaged over at least a 12-s acquisition (*simulator reference configuration*). At the therapy session, patients were fitted with the set of markers and they were manually positioned on the couch: operators were guided by two orthogonal laser lines intercepting semi-permanent tattoos on the subject's skin at CT time. The optical tracker was used to refine patient positioning by following, in real time (100 Hz), the displacements between the current marker configuration and the corresponding *simulator reference* one. EPID control was performed to check the final setup.

The retrospective data analysis aimed at evaluating the inter-fractional operator-dependent misalignments separate-

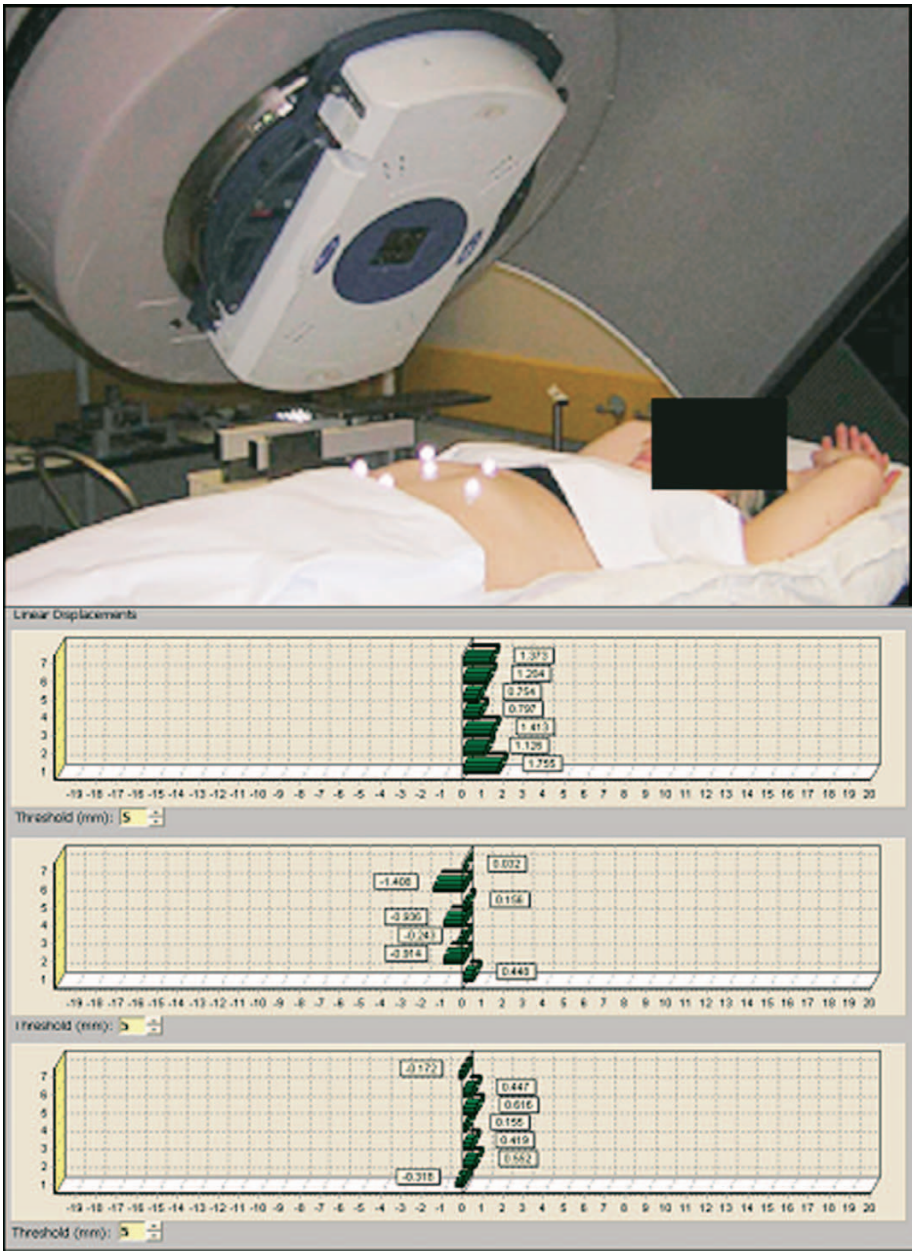

Fig. 1. *Upper panel:* Patient setup at the therapy unit. *Lower panel:* Shifts along the principal directions, computed and displayed by the opto electronic system.

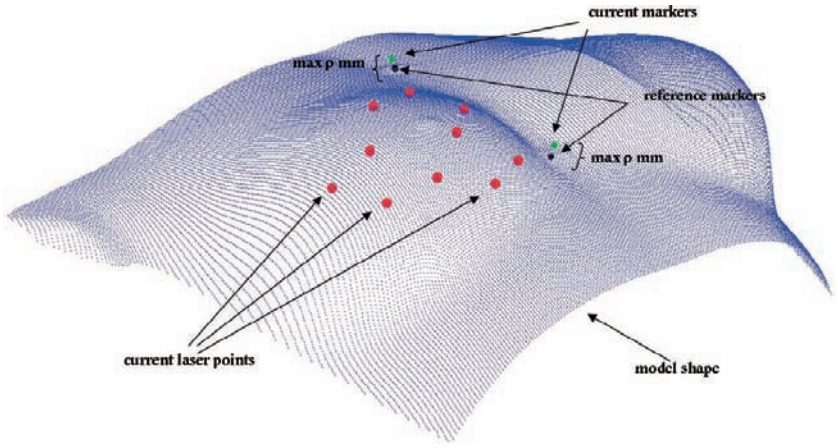

Fig. 2. Graphical representation of algorithm inputs.

ly from the influence of respiratory movements. The 3D position of control points was computed by averaging the optoelectronic frames that corresponded to only the patient's end of spontaneous expiration (*EE* frames). According to Baroni *et al.,*[6] *EE* frames were recognized as the relative minima of the breathing phase signal by means of two markers placed on the abdominal site. *Inter-fractional random errors* were assessed for each acquisition involving each patient, by averaging specific control point positions corresponding to *EE frames*, and by calculating the corresponding displacement with respect to the average patient specific reference position. *Peak position deviations* of the markers were quantified using the single frame of each acquisition that featured the highest overall root-mean-square displacement of the control points.

Surface-based Techniques for Patient Positioning: Hybrid Configuration of Control Points

Nine informed and consenting patients treated with post-operative external radiotherapy were enrolled in the study.[13] Patients were fitted with five infra-red reflective, radiopaque surface markers during the CT scans acquisition for treatment planning. Two markers (*fiducials*) were placed on the medio-sternal line and were used as *fiducials* for surface registration. The remaining three markers (*verification*) were placed close to the upper margin (UP), the center (CENTRE) and the lower margin (DOWN) of the irradiation field. The 3-D the surface model of the treated area was obtained from the CT dataset ,and the reference position of *fiducials* and *verification* points was identified by means of cross-correlation techniques. At each irradiation session, markers were replaced on the patient and a set of 9 laser spots were generated on patients breast surface. Markers and laser spots position were recorded in 3-D by a 2-TV camera opto-electronic localizer. The surface matching numerical procedure, which was used to evaluate the displacement between the current and the reference patient position, was based on the *Iterative Closest Point* algorithm.[14] A dedicated constrained version of the method was developed in order to increase convergence, where the constraints were the re-localization of the two passive markers (M1 and M2), used as fiducials, which were placed on the medio-sternal line in correspondence of the tattoos used for patient manual alignment.[15]

The algorithm was provided with the reference and current configuration of the two fiducial markers, with the point-based description of the 3-D surface model (*model shape*) and with the current 3-D laser spot coordinates (Fig. 2); the output was the 6-parameter rigid spatial transformation, which best interpreted the detected patient mispositioning.

Those parameters were used to simulate the improvement in patient setup, which would have been obtained by acting on the servo-controlled movements of treatment table and therapy unit. The position improvement was checked by evaluating the residual errors on the verification passive control points (UP, MED and DOWN) which were not included in the registration procedure.

Surface-based Techniques for Patient Positioning: Neural Network Approach

According to Frosio *et al.,*[16] the method was based on the CT breast surface model obtained from the treatment planning system. CT data for treatment planning of 4 subjects, enrolled in this study, were processed with a commercial software (Amira^{TM} 3.1.1, TGS Inc.), in order to reconstruct breast surface models. The configuration of laser spots on the surface model was defined by means of a simulated experimental setup of 10 laser beams. The generated laser spots in reference condition (*Virtual Markers*, VM_r) were considered solid with the 3D surface and used as verification points for the evaluation of the neural algorithm performances. A set of 10 Artificial Neural Networks (ANN, one for each laser spot) was trained to estimate the current 3D coordinates of *Virtual Markers* (VM_c) from the current laser

beams intersections (l_c) with the surface model. The ANN training dataset was generated by applying 2000 random 6-dofs rototranslations to the reference surface model. Range of linear and angular displacement was set to ±10 mm and ± 6°. For each model, two training dataset were generated: in the first case, no model deformations were considered (*undeformed* training); in the second case (*deformed* training), a geometrical surface deformation tool was implemented and applied to each model during the training, in order to mimic intra-session target motion and deformation due to patient breathing. Non-rigid deformation ranged from –8 mm (deep expiration) to 12 mm (deep inspiration) with respect to the mean respiration level. With the same modalities testing dataset was generated (*undeformed* testing and *deformed* testing).

In order to simulate patient position correction the ANN output was fed to an iterative procedure, which was designed to estimate the best set of roto-translation corrective movements (in a least-squares sense) for the minimization of the displacements between reference and ANN predicted current *Virtual Markers*. A brief sketch of the entire procedure is presented in Fig. 3.

The network performance was evaluated by computing the *root mean square error* between the desired and the networks estimated outputs. The model position correction after the application of minimization procedure was checked by calculating the residual errors on the estimated *VMc*.

Optimal Marker Configuration

Accurate correction of inner target displacements requires adequate selection of the external points configuration to gain effective reduction of the target displacements (target registration error, TRE).[17,18] TRE is a function of different factors, including the fiducial configuration, the number of fiducial markers, and the fiducial registration error (FRE). In current clinical practice, such aspects are hardly taken into account, and random marker configurations are exploited. Therefore, target positioning accuracy through opto-electronic localization systems would benefit from the application of methods to design optimal configuration of the sur-

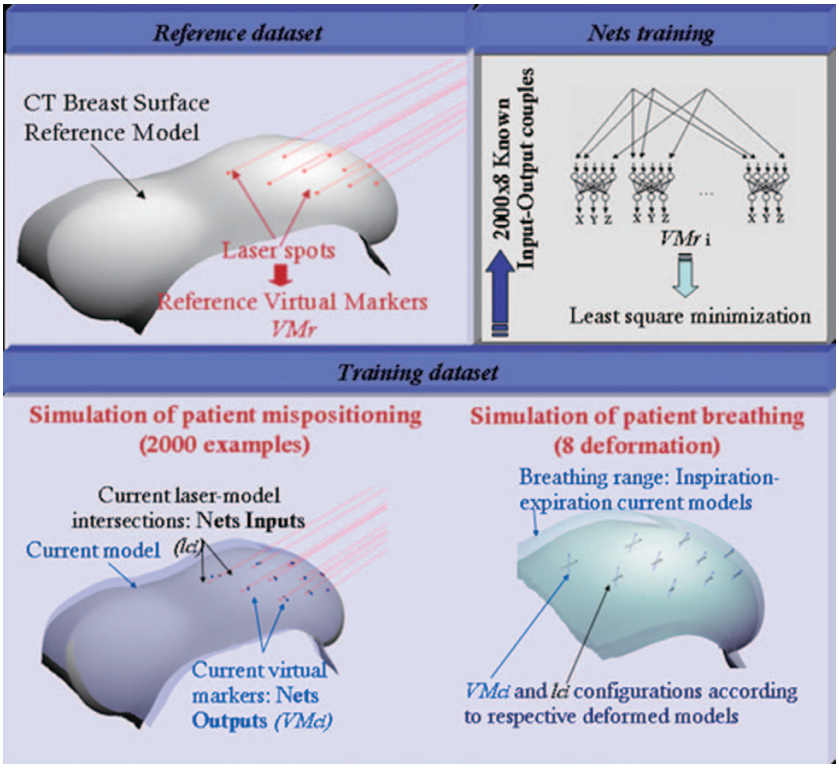

Fig. 3. The configuration of laser spots on the surface model was defined by means of a simulated experimental setup of 10 laser beams. The generated laser spots in reference conditions (VMr) were considered solid with the 3D surface and used as verification points for the evaluation of the neural algorithm performances (see upper left panel). The ANN training dataset was generated by applying 2000 random 6-dofs roto- translations to the reference surface model and 8 breathing deformation patterns (see lower panel). When undeformed model training was tested, the 8 model were not take into account. A set of 10 ANN (one for each laser spot) was trained to estimate the current 3D coordinates of Virtual Markers (VMc) from the current laser beams intersections (lc) with the surface model, which was displaced and deformed, according to simulated patient mispositioning and breathing movements, respectively.

face markers.

Genetic algorithms (GA) and taboo search (TS) were selected for the implementation of a newly designed non-deterministic algorithm, featuring enhanced capabilities of handling local minima in TRE optimization. In such algorithm, a population-based evolution, borrowed from GA, is generated,[18] where adaptive memory features guide the evolutionary process to thoroughly explore the solution space.[19] Those marker configurations resulting collinear from the point of view of infrared cameras are rejected relying on a predefined list of taboo solutions.

Treatment planning CT scans coming from 10 prostate patients were segmented to provide a spatially coherent 3-D representation of target, OARs and external skin surface Fig. 4. Planning data were fed to the algorithm in order to obtain optimized configurations of markers, to be compared to a random configuration.

The changes in the optimal marker configuration when prostate and bladder are considered target structures were also investigated through multiple runs of the optimization algorithm. According to conventional patient setup practice at the Radiotherapy Division of the European Institute of Oncology the overall number of markers was set to 7 in each optimization procedure,. Similarly, the marker visibility constraint was implemented assuming the 2-TVC configuration that is currently installed in the treatment room. The discrepancy between random and optimal configurations was assessed in terms of the spatial distribution of body markers onto the surface model. This was achieved by introducing the root mean square (RMS) distance between corresponding points as metric. Point correspondence between two different marker configurations was established on the basis of marker Euclidean distances (*closest point*).

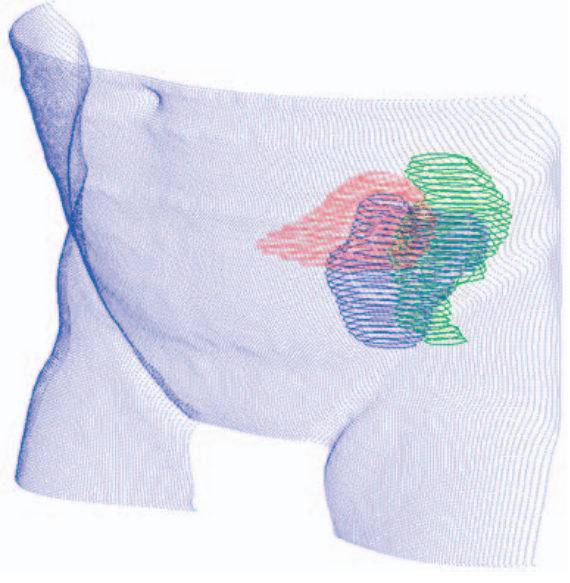

Fig. 4. Skin surface model of patient 1, showing in transparency the segmented target (prostate+seminal vesicles, in blue), bladder (red) and rectum (green).

Anatomical Calibration Techniques

A specific procedure for isocenter frameless localization and correction of patient setup was implemented.[9] In order to compensate both system noise and the inaccuracies in manual remarking procedures, each possible combination of fiducials featuring from 4 to 7 control points was considered, and local reference axes X_S, Y_S and Z_S were built for each subset S (see Fig. 5), according to the following guidelines:

- the orthogonal principal directions of the points are selected as local reference axes, so that redundancy in the evaluation of local coordinates is accounted for;
- the origin of the local reference system is positioned in the centre of mass (unweighted mean) of the configuration of control points.

Reference CT data allowed the definition of local coordinates of the isocenter $[\mathrm{xl\ yl\ zl}]_S$ for every subset S: the mapping of each triplet of local coordinates in the absolute reference system $[X_C\ Y_C\ Z_C]_S$ contributed to the final isocenter localization $[X_C\ Y_C\ Z_C]$ through a weighted mean, being w_S the weight of subset S:

$$\begin{bmatrix} X_c & Y_c & Z_c \end{bmatrix} = \frac{\sum_{\forall S} w_S \cdot \begin{bmatrix} X_s & Y_s & Z_s \end{bmatrix}}{\sum_{\forall S} w_S}$$

The value of w_S for each subset S was calculated as follows:

$$w_s = \frac{n_s}{\left\| \{\mathbf{f}_{r,l}\}_s - \{\mathbf{f}_{c,l}\}_s \right\|}$$

where n_S is the number of markers included in subset S, $\{\mathbf{f}_{r,l}\}_S$ and $\{\mathbf{f}_{c,l}\}_S$ represent their reference and current local coordinates and symbol $\| \ \|$ denotes the Euclidean norm.. Similarly, rotations Ω, Φ, and K between the current and reference configuration were evaluated through the weighted mean of relative angles Ω_S, Φ_S, and K_S concerning each subset.

In order to estimate the isocenter position repeatability and the automatic correction modalities in the frame of the reported patient positioning procedure, a specific analysis was performed through the algorithm for corrective parameters estimation previously described. The specific aim was to quantify the potential improvement of patient setup when patient breathing is an issue. Collected positioning data (46 patients treated with hypofractioned stereotactic radiation therapy) were analysed aiming at the extraction of the most significant frames in terms of surface breathing motion. A point-based registration between the current and reference positions of markers was applied, and each frame was scored depending on the residual fiducial registration error (FRE). The two frames exhibiting the highest (*High FRE*) and low-

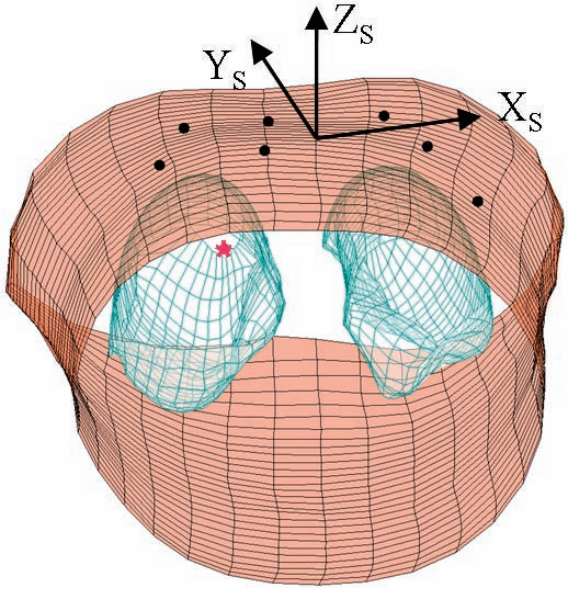

Fig. 5. Definition of the local reference system used for stereotactic localization. Local reference systems were exploited for the stereotactic reconstruction of tumor localization (symbol *).

est (*Low FRE*) FRE value were selected from each acquisition. The isocenter reconstruction procedure was tested in the two conditions (*Low FRE* and *High FRE*), providing the 3-D localization of the isocenter at minimum and maximum FRE value, respectively. The reproducibility in the 3-D localization of the centre of mass of the lesion was thus analysed, allowing the computation of the effects due to the occurred non-rigid deformations, indicated by *High FRE* vs. *Low FRE* values, on overall localization accuracy.

Moderate Deep Inspiration Breath Hold

When considering extra-cranial sites, intra-fractional variations are mainly due to patient breathing.[20,21] Respiration may result in target localization uncertainties that are definitely higher than the accuracy that is requested for high precision radiation therapy.[21]

The DIBH technique involves instructing the patient to reach and maintain the same, reproducible deep inspiration level (100% vital capacity) throughout the various phases of treatment planning and delivery.[22] This technique provides a double advantage: an increase in the positional repeatability of the target, by decreasing the respiration-induced variability, and the reduction of lung parenchyma density,[22] with a resulting minimization of the side effects for healthy tissues.[23,24]

Voluntary breath hold maneuvers can be performed with or without active systems for the on-line control of air flow. The applicability of moderate deep inspiration breath hold (mDIBH), where deep inspiration is limited to 75% vital capacity, aiming at improved patient comfort in breath hold execution, was purposely investigated.[25] Preliminary experimental activities were performed on patients, in order to investigate the feasibility of mDIBH, guided by the opto-electronic system, as a way to increase the reproducibility of extra-cranial target localization by means of surface fiducials.[26] The position reproducibility in LL and AP direction of seven markers placed on thoraco-abdominal (for the supine position) and dorso-lumbar (for the prone position) regions was assessed during opto-electronic guided mDIBH in six patients. In these preliminary activities, patients were trained to follow the operator instructions, in the framework of an audio feedback approach. The corresponding reproducibility of the position of the target volume was evaluated by acquiring a CT scan (3 *mm* slices) at free breathing (FB) and two to three opto-electronic guided mDIBH CT scans (20 slices) centered on the lesion.

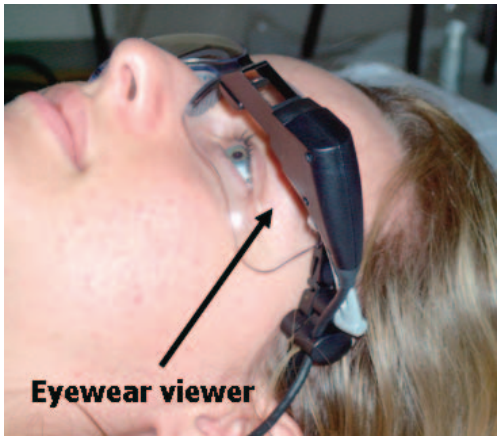

Fig. 6. The eyewear viewer, mounted on neutral glasses, utilized for video feedback.

Following these preliminary experiments, the mDIBH technique, monitored by the opto-electronic system ELITE, was clinically implemented for body stereotactic treatments. The clinical evaluation was performed on a 8 patients group, treated for extracranial lesions by means of hypo-fractionated dose delivery. Real-time visual feedback, providing instantaneous (at ~30 Hz video refresh rate) information of the inspiration level to the patient, was exploited to ensure maximal repeatability between consecutive breath holds. Visual feedback was provided by means of an eyewear viewer (SV-6 PC Viewer, MicroOptical Co., Westwood, MA), showing marker displacements in all directions as bars (Fig. 6).

Breath hold helical CT scans were split into mDIBH segments of 15 *s* each, while a free-breathing scan was also acquired for treatment planning comparison and patient setup. An independent opto-electronic localizer (ExacTrac®, BrainLAB A.G., Heimstetten, Germany) was utilized for patient setup evaluation during treatment. The system was used to acquire the 3-D coordinates of external markers during the execution of breath hold maneuvers. Furthermore,

the system provided 3-D localization of treatment isocenter by means of a proprietary method for stereotactic localization based on surface markers.

Real Time Tumor Tracking in High Precision Radiotherapy

ANN-based algorithms for the real-time tumour tracking in lung high precision radiotherapy were developed and tested. The design was optimized on specific data coming from simulations with a 4D nurbs-based numerical phantom for 4D CT data generation, NCAT 4D 1.13.[27] By means of this tool, it was possible to generate a virtual anthropomorphic phantom including liver or lung lesions (Fig. 7). The inner organ shapes of the phantom (lungs, heart, stomach, liver, kidneys and spleen) were designed using superficial NURBS (non-uniform rational b-splines).

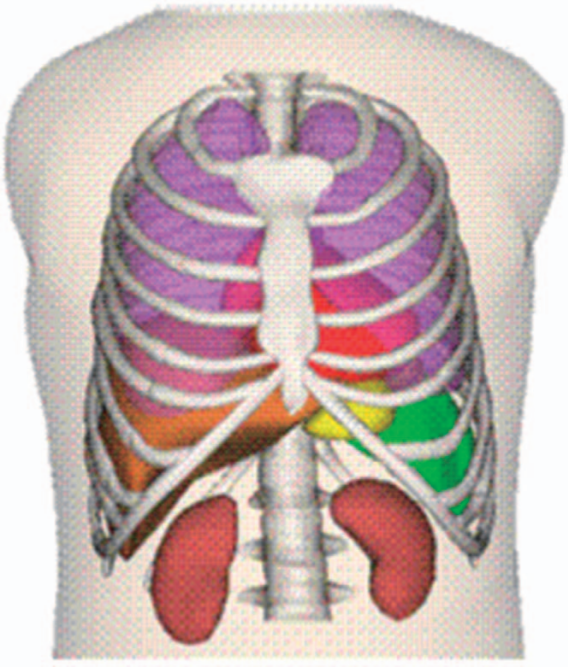

Fig. 7. The digital human phantom generated from NCAT software (*figure courtesy of Paul Segars*).

The morphology of the skeleton and the organs of the thorax (except heart) was based on CT scanning of the Visible Human Project® data-set. As a consequence, a digital phantom that reproduces the anatomical structures and the cardiac and respiratory movements of a normal human subject was obtained. Different datasets were created by modifying the following parameters: tumor position and dimension; subject size and genre (male and female); patient position (prone and supine); phase/amplitude of the breathing pattern. Datasets consisted of a series of 4D CT images, of the 3D trajectory of tumor center of mass and of the 3D trajectory of an internal point close to diaphragm. A neural network was trained to predict the movement of tumor (net output) starting from the diaphragm motion (net input). The training breathing dataset included three different respiratory cycles with different amplitude and frequency as well as the testing one. Once trained, the implemented ANN-based approach can supply immediate output (tumor motion) as a function of the input: the limiting factor in terms of global throughput is given by the acquisition rate of input data.

RESULTS

Optical Point-based Techniques for Patient Position Monitoring

The frequency distribution of linear and 3D-size of the inter-fractional random errors affecting external control points is showed in figure 8 (*left panel*). Results are relative to data analysis with breathing movement compensation. Statistical dispersion of point misalignments (± 2 SD) turned out to be fairly small being within a range of ± 3.2, ± 3.8, and ± 3.4 mm along the lateral, cranio-caudal, and antero-posterior directions, respectively. The corresponding distribution of the 3D displacements exhibited an overall median ± quartile value of 2.6 ± 1.8 mm, with 95% of the observed cases (95th percentile) within 5.0 mm. Statistics (non parametric comparison of two independent groups) revealed slightly significant differences between 3D displacements in the supine and prone position ($p \leq 0.03$) with median ± quartile values of 2.5 ± 1.7mm and 2.9 ± 2.3mm, respectively.

The effect of breathing movements is reported in Fig. 8 (*right panel*) which shows the frequency distribution histograms of the linear and the 3D *peak position deviation* affecting the external control points. Position reproducibility along the antero-posterior direction was significantly affected by respiration, being 90% of the observed cases (5th–95th percentile) within ± 2.2 mm and ± 7.2 mm. The median ± quartile value of the corresponding 3D displacements increased to 3.6 ± 2.6 mm, with 95% of the observed cases (95th percentile) within 7.0 mm.

Surface-based Techniques for Patient Positioning: Hybrid Configuration of Control Points

Statistical analysis was performed on the initial marker displacements, in order to evaluate the efficacy of conventional manual patient positioning in the clinical practise of breast radiotherapy. Kruskal-Wallis Anova test, with displacement direction (latero-lateral, cranio-caudal, antero-posterior) as independent variable, revealed significant differences on the initial displacements of passive markers. Scheff test showed that the errors along the antero-posterior direction were significantly preponderant ($p < 10^{-5}$) with respect to misalignments along the remaining directions. The second step consisted in appraising ICP algorithm performance, by comparing 3-D initial and residual displacement of the two fiducial and the three verification control

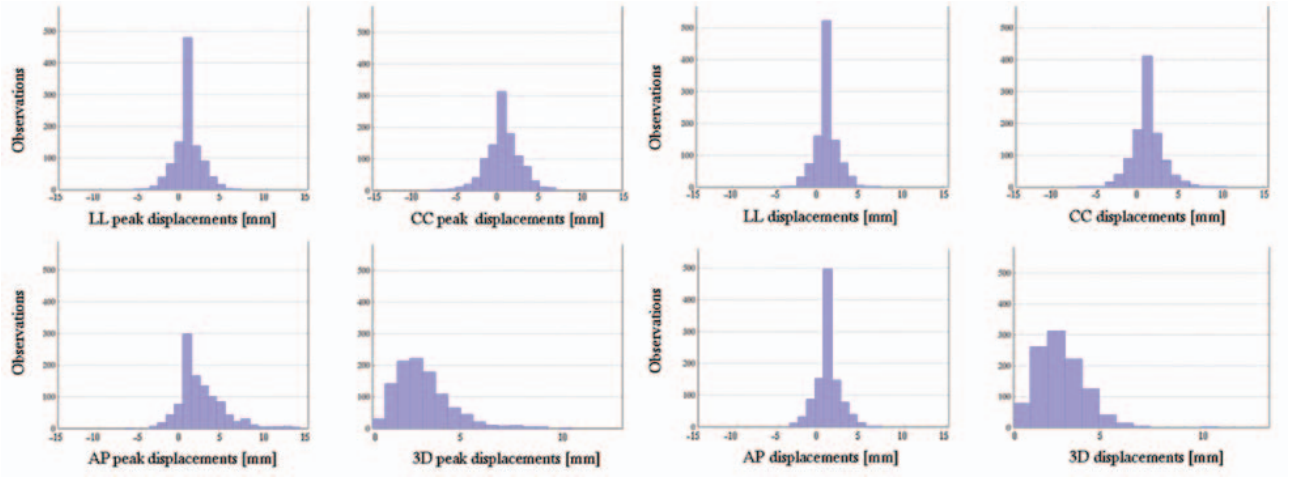

Fig. 8. *Right panel:* Frequency distribution plots of the linear and the three-dimensional displacements of the external control points, obtained with compensation of breathing movements. *Left panel:* Frequency plots of peak errors, thus including effects of breathing movements.

points. In average, the mean value of the relocalization value on the two medio-sternal control points was enlarged to 3.18 mm. This increased the level of convergence of the constrained registration algorithm and brought to residual errors affecting the verification points (UP, MED and DOWN) after position correction reported in Fig. 9 (dark bars).

Median values of initial displacements of control markers (UP, MED, DOWN) were 5.59 mm, 6.15 mm, 4.98 mm respectively. After correction simulation, these were reduced to 3.91 mm (UP), 3.27 mm (MED), 3.42 mm (DOWN). Data variability (75th percentile) (7.89 mm, 7.21 mm, 6.37 mm before correction, 3.56 mm 5.04 mm and 4.59 mm after correction) as well as peak values (13.35 mm, 10.89 mm, 13.06 mm before correction, 7.62 mm, 7.93 mm and 8.21 mm after correction) were also consistently reduced. Wilcoxon signed rank test for pair data validated significant 3-D displacements reductions for markers UP ($Z = 8.12$, $p < 1e\text{-}6$), MED ($Z = 9.21$, $p < 1e\text{-}6$) and DOWN ($Z = 5{,}80$, $p < 1e\text{-}6$).

Surface-based Techniques for Patient Positioning: Neural Network Approach

ANN performances were evaluated by calculating the *root mean square error* between desired outputs and networks predicted outputs. RMSE was decomposed in its random (RMSEr) and systematic (RMSEs) component, being this latter related to possible algorithm bias. RMSE values, in the case of mean level of respiration, were 2.56, 3.79, 3.28 and 1.89 mm for patient 1, 2, 3 and 4, respectively, with a very low systematic component (0.81, 0.92, 0.73 and 1.14 mm). Fig. 10 shows *median* ± *quartile* values, computed on the 100 testing examples, of initial and residual 3-D displacements affecting control points of patient 2 and patient 4, which were the worst and the best case respectively for *undeformed* testing. Displacements on control points were always brought down below 5 mm up to the 75th percentile even when deformation was included in the training dataset. Wilcoxon ,signed rank test for pair data confirmed signifi-

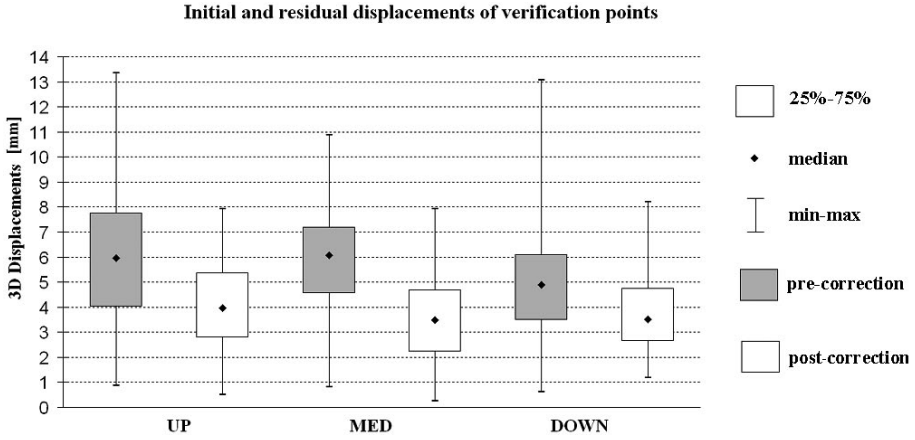

Fig. 9. Comparison between 3-D initial and residual displacements of the three verification points (UP, MED, DOWN).

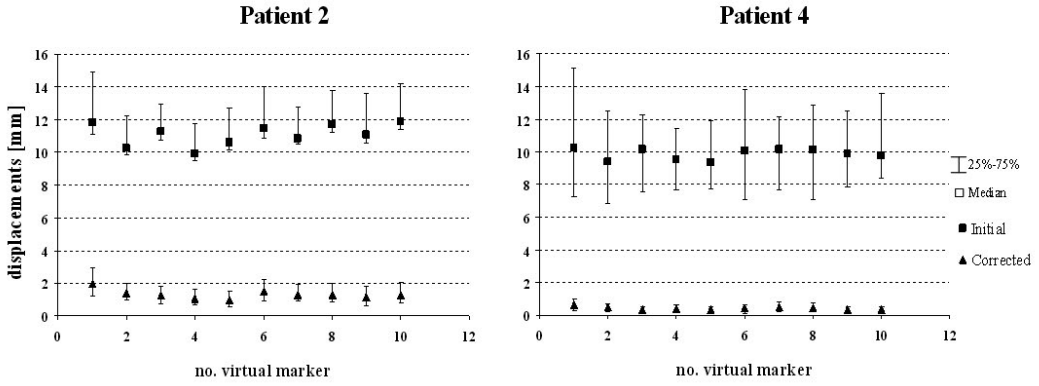

Fig. 10. Three dimensional setup errors on Virtual Markers before and after correction (undeformed model testing).

cant 3-D displacements reductions for virtual markers with $p < 1e\text{-}6$.

Optimal Marker Configuration

The stochastic algorithm yielded a significant improvement of TRE/FRE ratio for the optimal vs. random marker configuration (26.5% mean decrease). When considering the whole simulation dataset, optimized configurations exhibited a mean TRE/FRE ratio measuring 0.49 (range 0.47–0.51), vs. 0.67 (range 0.59–0.74) for random configurations.

Optimal marker configurations turned out to have a typical optimized spatial distribution thus highlighting common features 10 patients group. Optimized solutions are characterized by an approximately symmetric distribution, where markers are mostly placed on lateral sides, close to the limit of TVC field of view.

Optimal marker configurations when OARs were included among target structures exhibited a mean increase in TRE/FRE ratio measuring 1.9%, with respect to the PTV-only condition. This was confirmed by non parametric statistic comparison (Mann-Whitney test), that revealed a significant difference in TRE/FRE values ($p = 0.0017$). Similarly to the optimum vs. random configuration comparison, similarities in the optimal configuration was assessed through the RMS distance between homologous points. OARs inclusion often resulted in a similar but symmetric optimal configuration, if compared to the PTV-only condition. This is due to the fact that skin surface models feature a mirror symmetry, with respect to the sagittal plane. RMS discrepancies in the optimal configurations, evaluated in the point-based metric were (mean ± SD) 33.9 ± 16.9 *mm*. This signifies a much higher similarity than the one highlighted in the optimum vs. random configuration comparison, being the measured RMS distance (mean ± SD) 124.0 ± 14.7 *mm* in this case.

Repeated simulations (3 for each patient) revealed comparable values of TRE/FRE ratio. No significant difference (Friedman ANOVA test) was found when comparing TRE/FRE values corresponding to different runs of the algorithm (99% confidence). The comparison of optimal solutions in the point-based metric revealed a RMS repeatability in marker spatial distributions measuring (mean ± SD) 34.9 ± 19.8 *mm*.

Anatomical Calibration Techniques

Fig. 11 depicts the 3-D localization of the isocenter, which was reconstructed in the first fraction of the 46 considered patients. Results show a slight lower variability of isocenter localization in *Low FRE* condition, if compared with the *High FRE* condition.

The isocentric positioning correction was also applied, simulating a 6 degrees of freedom optimisation of patient position, in order to quantify the expected improvement in the geometrical setup by means of marker 3-D displacements. Initial and residual displacements of markers position, evaluated before and after the application of the implemented correction procedure, were evaluated in the two *FRE*-dependent conditions at each irradiation session. The isocentric positioning correction provided a reduction of median values in the *Low FRE* condition up to 2.9 *mm* (Fig. 12). A more considerable improvement in residual marker displacement was obtained in the *High FRE* condition, with a decrease in median values measuring 3.2 *mm*

It is also important to underline that, according to the modality of corrective parameters estimation, the reported residual displacements affecting the external markers are coupled with a nominal perfect correction of the isocenter.

Moderate Deep Inspiration Breath hold

Results in the preliminary phase showed that, during the execution of a single 15 *s* mDIBH maneuver (intra-mDIBH), surface marker displacements (1SD) ranged from 0.6 to 1.3 *mm* in LL direction and from 1.0 to 1.8 *mm* in AP direction. The reproducibility of marker position between different mDIBH maneuvers was affected by RMS errors lower than 1.9 and 2.2 *mm* in LL and AP directions, respectively. These results were found to be highly correlated with data of GTV

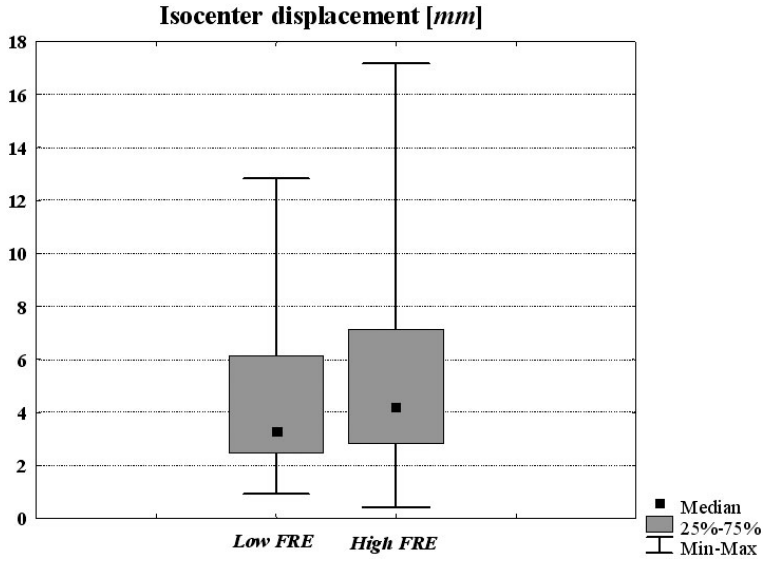

Fig. 11. Frameless isocenter localization before correction, at the minimum of fiducial registration error (*Low FRE*), and in correspondence of the peak external markers deviation with respect to the reference configuration (*High FRE*).

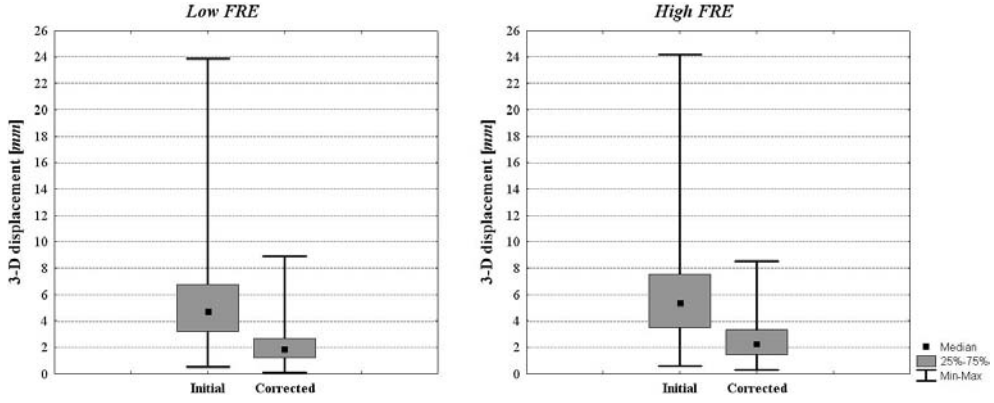

Fig. 12. Markers displacements before and after the 6 dofs corrective procedure. *Left*: initial and residual displacements in the *Low FRE* condition; *Right*: initial and residual displacement in the *High FRE* condition (including breathing movements).

position reproducibility, which revealed mean variations of 0.9, 1.0 and 1.7 *mm* in LL, AP and CC directions.

The application of mDIBH maneuvers turned out to allow average reduction of PTV volumes for all patients, with respect to free-breathing (1-*cm* isotropic margin), up to 28.4%. An example of co-registered FB and mDIBH CT scans is depicted in Fig. 13. Clinical results show a significant increase in lung volume and reduction of PTV relatively to normal breathing, thus reducing the fraction of normal lung tissue irradiated. This confirmed the potentialities of mDIBH treatments already highlighted in the preliminary CT study. Visual feedback of marker displacements led to a high reproducible surface localization during mDIBH maneuvers. Inter-mDIBH reproducibility, measured during the acquisition of the helical CT scan, measured (mean ± SD) 1.1 ± 0.5 *mm* and 2.0 ± 0.3 *mm* in LL and AP directions, respectively. The corresponding intra-mDIBH variability was even smaller, being 0.3 ± 0.1 *mm* in LL direction and 0.9 ± 0.4 *mm* in AP direction. Inter- and intra-mDIBH reproducibility, evaluated over the course of treatment, is reported in Table 1, where data concerning external markers and treatment isocenter are reported. It is worth stressing that these results were independently provided by the ExacTrac system, that was not used to supply visual feedback to the patient.

Higher confidence with this procedure will lead to a reduction of CTV to PTV margins. Breath hold monitored by an opto-electronic system provided a simple and non invasive method to minimize breathing motion for collaborative and trained patients. Nevertheless, the need for active

patient compliance and good respiratory functionality appears as a limitation of the procedure.

Real Time Tumor Tracking in High Precision Radiotherapy

The ANN-based approach revealed good performance in tumor trajectory estimation. In Fig. 14 ANN-based tumor trajectory (blue) vs. ground truth tumor motion (red) is shown for the worst (left) and the best case (right). The respective root mean square errors were 0.46 mm in the first case and 0.02 mm in the second case. Best results were found when in the training data set many different respiratory patterns were included, by varying both amplitude and frequency of breathing cycle.

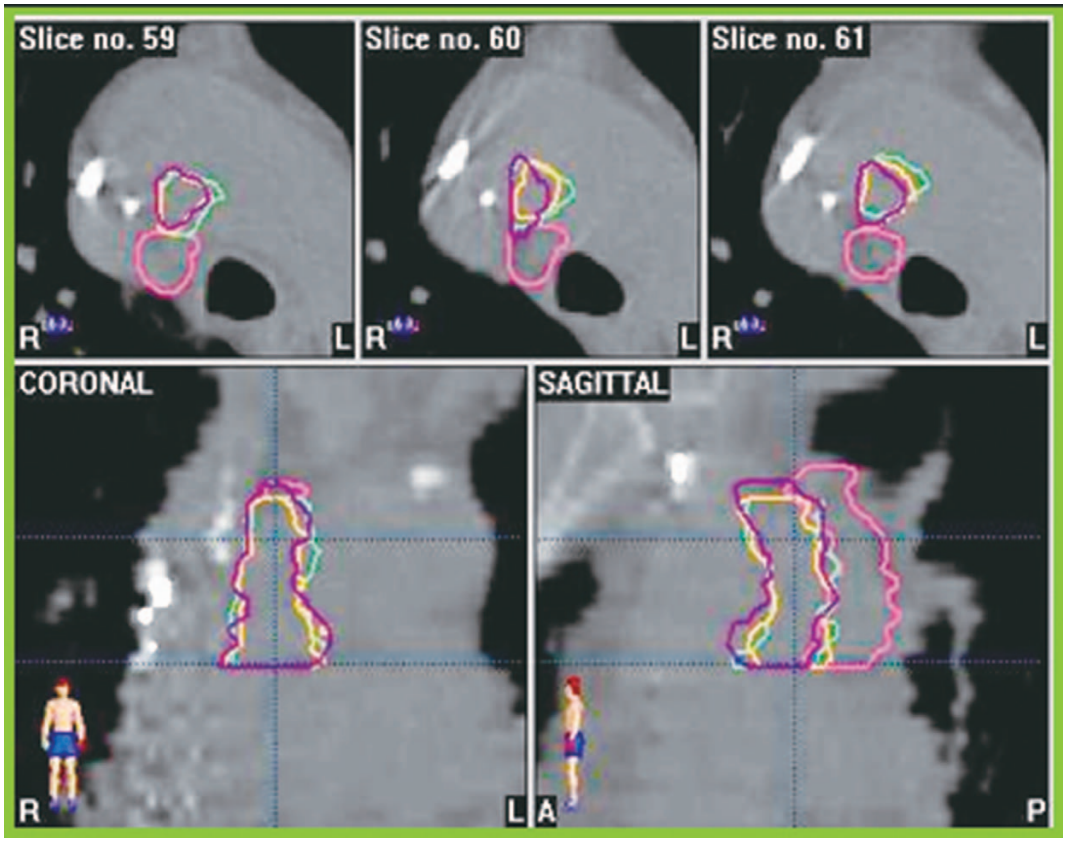

Fig. 13. Multiple views of the registered CT scans dataset for patient 3 (mediastinic lymph node). Tumor location at FB (pink contour) exhibits a significant displacement from the three mDIBH contours, depicted in violet, yellow and green, respectively.

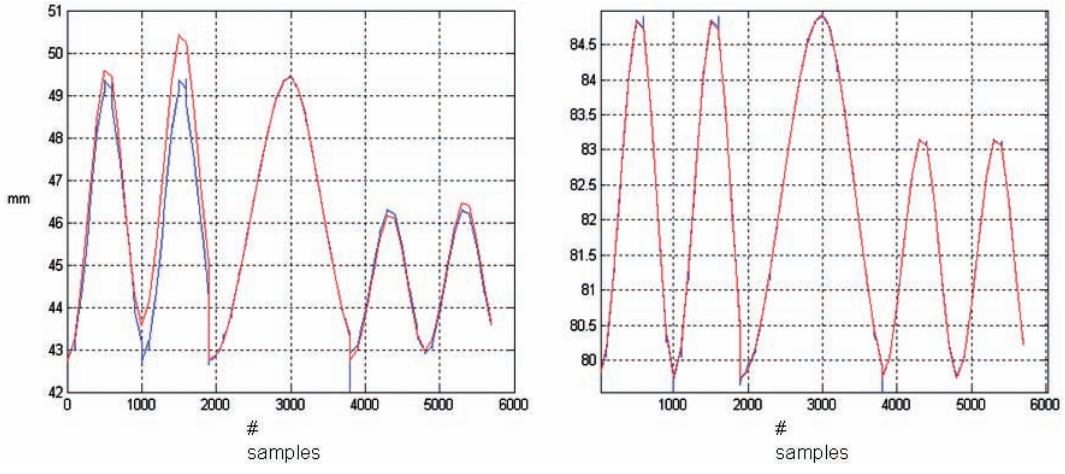

Fig. 14. Graphical comparison of the desired (red) and estimated (blue) tumor trajectory along the antero-posterior direction.

DISCUSSION

Optical tracking techniques revealed high performance in patient setup and monitoring in external beam radiotherapy. Conventional techniques for patient positioning may lead to unacceptable deviations in the planned radiation dose distribution, thus undermining the potential benefits of highly conformal treatments.[28] The systematic application of optical tracking technologies significantly increases the repeatability in daily patient setup, and provides quantitative documentation of treatment quality. Nevertheless, a much more aware exploitation of such technologies is needed for the effective reduction of target localization errors, in the framework of a rigid body registration approach.

In particular, when point-based methods are utilized, robust procedures for the compensation of soft tissue artifacts in target position estimation have to be applied. Furthermore, external markers need to be conveniently placed onto the skin surface in optimized configurations: this is the necessary premise for actual target registration error minimization in patient setup. Given the high complexity of optimal marker placement estimation, non deterministic techniques, enhancing the capabilities of conventional optimization algorithms in exploring the solution space, have to be implemented.

The performed experimental and clinical testing of surface-based localization methods revealed that redundant information on surface topology is a valid alternative to conventional point-based registration. Surface-based methods exhibited adequate performance in detecting and monitoring surface deformation from day to day. Notwithstanding this, surface localization relying on thousands of points lacks in real-time monitoring capabilities, which is one of the main advantages of conventional point-based methods. Hybrid registration and ANN-based solutions ensured a good trade-off between redundancy and computational costs, emerging as a promising approach to be customized on site and patient-specific surface morphology.

The intrinsic features of surface-based methods suggest they should be preferred at those sites where deformation is an issue (e.g. breast), and for treatment techniques requiring adequate monitoring of the entrance surface (particle therapy). Caveats apply in the use of such methodology when surface topology has insufficient spatial frequency, out of multiple local minima in the surface fitting process. In this case, hybrid techniques may play a decisive role, combining surface monitoring capabilities with enhanced interpretation of the spatial relationships between smoothly shaped surfaces.

Whereas the described use of point- and surface-based methods is meant to reduce patient setup errors, the minimization of organ motion uncertainties in tumor targeting can be achieved through the application of specific clinical protocols. The intrinsically different nature of inter-fractional vs. intra-fractional organ motion events makes this purpose extremely challenging, as diversified solutions need to be implemented. Breath hold techniques have been successfully applied for the compensation of and intra-fractional organ motion. Nonetheless, point- and surface-based localization have to be integrated with these protocols for setup monitoring on one hand, and breathing phase detection on the other. This combined approach represents the basic methodological rationale for the contemporary reduction of setup and internal margins, thus leading to higher selectivity in radiation dose administration.

Future developments are needed for a deeper understanding of the non linear correlation between internal and external features at different anatomical sites. Modern IGRT technologies for in room image guidance (orthogonal X-rays, cone beam CT, ultrasound) yield sufficient data for site and patient-specific evaluations of such correlation. This represents a necessary step toward the individuation of reliable anatomical calibration models, overcoming the limitations of the currently adopted rigid body assumption. Innovative anatomical calibration models are supposed to include a mathematical representation of site-specific organ motion events, to be correlated to a convenient set of external (points, surfaces) features. The validation of such models could provide in the future the implementation of real-time tumor targeting packages based on non invasive point and surface-based technologies.

The systematic use of optical tracking technologies is put forward to represent a significant increase in the accuracy of treatment delivery, when fully integrated with specific in-room imaging procedures. In order to take into account both positioning (SM) and organ motion (IM) uncertainties in patient setup, the following twofold approach is proposed:

1. minimization of setup margin SM through the real-time verification and correction of patient misalignments, with reference to an external configuration of features (points and surfaces) to be optimized according to patient-specific treatment planning data
2. optimization of internal margin IM by accounting for organ motion and soft tissue deformation relative to the external references. This purpose is achieved by means of appropriate data analysis, integration with IGRT technologies, and by means of specific protocols for detecting and compensating organ motion events.

In this perspective, external features do not simply represent distant surrogates of the CTV, even in case mobile structures are targeted. Quantitative external localization allows one to count on a precisely localized sheath wrapping the mobile target, as well as to estimate the position of the CTV, once organ motion events have been measured in an IGRT approach. This is essential to adequately spare stable critical structures, which are far from the CTV but close to the radiation beam pathways, to improve the adequacy of prior established PTV. Furthermore, one can count on a real-time

monitored anatomic reference, with respect to which target relative displacements can be modeled, measured, and compensated with less effort and higher reliability.

REFERENCES

1. Timmerman, R Papiez, L. and Suntharalingam, M. (2003) Extracranial stereotactic radiation delivery: expansion of technology beyond the brain. Technol. Cancer. Res. Treat. **2**: 153–160.
2. Murphy, M. J. (2002) Fiducial-based targeting accuracy for external-beam radiotherapy. Med. Phys. **29**: 334–344.
3. van Herk, M. (2004) Errors and margins in radiotherapy. Semin. Radiat. Oncol. **14**: 52–64.
4. Baroni, G., Garibaldi, C., Scabini, M., Riboldi M., Catalano, G., Tosi, G., Orecchia, R. and Pedotti, A. (2004) Dosimetric effects within target and organs at risk of interfractional patient mispositioning in left breast cancer radiotherapy. Int. J. Radiat. Oncol., Biol., Phys. **59**: 861–871.
5. Baroni, G., Ferrigno, G., Orecchia, R. and Pedotti, A. (2000) Real-time opto-electronic verification of patient position in breast cancer radiotherapy. Comput. Aided Surg. **5**: 296–306.
6. Baroni, G., Ferrigno, G., Orecchia, R. and Pedotti, A. (2000) Real-time three-dimensional motion analysis for patient positioning verification. Radiother. Oncol. **54**: 21–27.
7. Jaffray, D. A. (2005) Emergent technologies for 3-dimensional image-guided radiation delivery. Semin. Radiat. O8. ncol. **15**: 208–216.
8. Meeks, S. L., Tome, W. A., Willoughby, T. R., Kupelian, P. A., Wagner, T. H., Buatti, J. M. and Bova, F. J. (2005) Optically guided patient positioning techniques. Semin. Radiat. Oncol. **15**: 192–201.
9. Riboldi, M., Baroni, G., Spadea, M. F., Bassanini, F., Tagaste, B., Garibaldi, C., Orecchia, R. and Pedotti, A. (2006) Robust frameless stereotactic localization in extra-cranial radiotherapy. Med. Phys. **33**: 1141–1152.
10. Bert, C., Metheany, K. G., Doppke, K. and Chen, G. T. (2005) A phantom evaluation of a stereo-vision surface imaging system for radiotherapy patient setup. Med. Phys. **32**: 2753–2762.
11. Djajaputra, D. and Li, S. (2005) Real-time 3D surface-image-guided beam setup in radiotherapy of breast cancer. Med. Phys. **32**: 65–75.
12. Baroni, G., Garibaldi, C., Riboldi, M., Spadea, M. F., Catalano, G., Tagaste B., Tosi, G., Orecchia R. and Pedotti, A. (2006) 3D optoelectronic analysis of interfractional patient setup variability in frameless extracranial stereotactic radiotherapy. Int. J. Radiat. Oncol., Biol., Phys. **64**: 635–642.
13. Spadea, M. F., Baroni, G., Riboldi, M., Tagaste, B., Garibaldi, C., Orecchia, R. and Pedotti, A. (2006) Patient set-up verification by infrared optical localization and body surface sensing in breast radiation therapy. Radiother. Oncol. **79**: 170–178.
14. Besl, P. J. and McKay, W. D. (1992) A method for registration of 3D shapes. IEEE Trans. Patt. Anal. Mach. Intell. **14**: 239–256.
15. Riboldi, M., Baroni, G., Orecchia, R. and Pedotti, A. (2004) Enhanced surface registration techniques for patient positioning control in breast cancer radiotherapy. Technol. Cancer. Res. Treat. **3**: 51–58.
16. Frosio, I., Spadea, M. F., De Momi, E., Riboldi, M., Baroni, G., Ferrigno, G., Orecchia, R. and Pedotti, A. (2006) A neural network based method for optical patient set-up registration in breast radiotherapy. Ann. Biomed. Eng. **34**: 677–86.
17. Fitzpatrick, J. M., West, J. B. and Maurer, C. R. Jr. (1998) Predicting error in rigid-body point-based registration. IEEE Trans. Med. Imaging. **17**: 694–702.
18. Liu, H., Yu, Y., Schell, M. C., O'Dell, W. G., Ruo, R. and Okunieff, P. (2003) Optimal marker placement in photogrammetry patient positioning system. Med. Phys. **30**: 103–110.
19. Glover, F. (1986) Future paths for integer programming and links to artificial intelligence. Comput Oper. Res. **13**: 533–549.
20. Langen, KM. and Jones, D. T. (2001) Organ motion and its management. Int. J. Radiat. Oncol., Biol., Phys. **50**: 265–278.
21. Shirato, H., Seppenwoolde, Y., Kitamura, K., Onimura, R. and Shimizu, S., (2004) Intrafractional tumor motion: lung and liver. Semin. Radiat. Oncol. **14**: 10–18.
22. Hanley, J., Debois, M. M., Mah, D., Mageras, G. S., Raben, A., Rosenzweig, K., Mychalczak, B., Schwartz, L. H., Gloeggler, P. J., Lutz, W., Ling, C. C., Leibel, S. A., Fuks, Z. and Kutcher, G. J. (1999) Deep inspiration breath-hold technique for lung tumors: the potential value of target immobilization and reduced lung density in dose escalation. Int. J. Radiat. Oncol., Biol., Phys. **45**: 603–611.
23. Kutcher, G. J., Burman, C., Brewster, L., Goitein, M. and Mohan, R. (1991) Histogram reduction method for calculating complication probabilities for three dimensional treatment planning evaluations. Int. J. Radiat. Oncol., Biol., Phys. **21**: 137–146.
24. Lyman, J. T. (1985) Complication probability as assessed from dose-volume histograms. Radiat Res. **104**: 13–19.
25. Garibaldi, C., Baroni, G., Riboldi, M., Tagaste, B., Catalano, G., Ciocca, M., Pedotti, A., Tosi, G. and Orecchia, R. (2003) Breath hold technique guided by an opto-electronic system for body stereotactic treatments: a feasibility study. Radiother. Oncol. **68**: S45–S46.
26. Riboldi, M., Garibaldi, C., Baroni, G., Spadea, M. F., Tagaste, B., Catalano, G., Orecchia, R., Bettinardi, V., Rizzo, G., Messa, C., Fazio, F. and Pedotti, A. (2004) Extracranial frameless stereotactic radiosurgery with multi-modal imaging and opto-electronic position verification. Elsevier International Congress Series **1268**: 318–322.
27. Segars, W. P. (2001) Development and Application of the New Dynamic NURBS-based Cardiac-Torso (NCAT) Phantom. Ph. D. Dissertation, The University of North Carolina.
28. Baroni, G., Troia, A., Riboldi, M., Orecchia, R., Ferrigno, G. and Pedotti, A. (2003) Evaluation of methods for opto-electronic body surface sensing applied to patient position control in breast radiation therapy. Med. Biol. Eng. Comput. **41**: 679–688.

Received on January 30, 2007
Revision received on February 27, 2007
Accepted on February 27, 2007